Research on the Rotational Accuracy of Aerostatic Spindle Under Variable Load Conditions

Jiawei YANG*, Tao GONG**, Li GUO***, Hongchun LI****, Jian WANG****, Ming ZHAO*****, Zhuangzhi LI******

*Hunan Yujing Machinery Co., Ltd., Yiyang, 413000, China, E-mail: jiaweiy0228@hnyj-cn.com
**School of Mechanical Engineering and Mechanics, Xiangtan University, Xiangtan, 411105, China,
E-mail: gongtao527164@163 (Corresponding Author)

***Hunan Yujing Machinery Co., Ltd., Yiyang, 413000, China, E-mail: 18397526764@163.com

****Hunan Yujing Machinery Co., Ltd., Yiyang, 413054, China, E-mail: 2013448@hnyj-cn.com

*****College of Mechanical and Vehicle Engineering, Hunan University, Changsha, 410082, China, E-mail: jw ang@163.com

******Hunan Yujing Machinery Co., Ltd., Yiyang, 4130000, China, E-mail: zm_dlpu@163.com ******Hunan Yujing Machinery Co., Ltd., Yiyang, 413000, China, E-mail: cuohui264@163.com https://doi.org/10.5755/j02.mech.41749

1 Introduction

The ultra precision machining machine tool is a type of ultra precision machining technology, which achieves nanometer level surface roughness and submicron level shape accuracy [1]. The aerostatic spindle is an important functional component, which affects machining accuracy. The aerostatic spindle is widely used in the field of ultra precision equipment manufacturing due to its advantages of high rotational accuracy, low friction power consumption, wide speed range, no pollution, and long service life [2]. The rotational trajectory of the aerostatic spindle is a manifestation of the rotational accuracy. The vibration amplitude and vibration mode of the aerostatic spindle can be explained by the axis motion trajectory. In the actual machining process, the rotational speed of the aerostatic spindle, the unbalanced mass of the rotor, and the impact load have a significant impact on the rotational accuracy. Specifically, impact loads can cause fluctuations in the vibration amplitude and equilibrium position of the rotor, resulting in complex dynamic responses and severely affecting the rotational accuracy of the spindle. Therefore, this study investigates the influence of periodic and impact loads on the rotational accuracy of the aerostatic spindle.

The rotational accuracy of the aerostatic spindle is affected by periodic or impact loads during the actual machining process. Lei et al. [3] established a dynamic model of a high-speed aerostatic bearing rotor system by solving the transient Reynolds equation, flow balance equation, and rotor motion equation to analyze the nonlinear effects of operating parameters on the rotor axis trajectory. Ding et al. [4] established a dynamic model of a rigid rotor system supported by gas static pressure bearings to study the influence of the number and position of small orifice throttling devices on the stability of the rotor system. Zhang et al. [5] studied supply pressure and rotational speed on the nonlinear behaviors of the aerostatic bearing-rotor system, based on the bifurcation diagram, orbit of rotor, frequency spectrum diagram, Poincaré map and speed waterfall diagram. Cappa et al. [6] investigated the influence of several manufacturing errors, bearing parameters and feeding geometries on the radial error motion of an aerostatic journal bearing. Yin et al. [7] established the aerostatic spindle dynamic model, which

used a finite element method and the Runge-Kutta fourth order method to solve the transient Reynolds equation and the rotor dynamics equations simultaneously for the dynamic response analysis of the rotor. Chen et al. [8] investigated the impact of velocity effects on the vibration characteristics and rotational accuracy of aerostatic spindles, a bearing-rotor system dynamics model based on velocity effects was established. Sun et al. [9] established a model based on the roundness error and unbalanced mass to explain and predict the radial synchronous error. The quantitative relationship between the bearing capacity of the air film and roundness error of the rotor is obtained by CFD. Shimada et al. [10] developed a method to numerically calculate the trajectory of the spindle rotator, supported by aerostatic bearings. The method was developed to numerically investigate and determine the effects on the rotational accuracy of the spindle during end milling when the cutting force is applied to the rotating rotor. Shi et al. [11] constructed the dynamic model of the whole aerostatic spindle, considered the effect of shaft tilt motion due to elastic deformation on the dynamic characteristics of the aerostatic bearing.

The above literature has analyzed the influence of bearing parameters, working parameters, and machining accuracy on the stability of the rotor system, but has not yet considered the impact of cutting loads and impact loads, on the rotational accuracy of spindle. In order to consider the analysis of the rotational accuracy under transient machining loads, a dynamic mathematical model of the aerostatic spindle rotor based on the transient compressible gas Reynolds equation and throttling parameters would be established. The Euler iteration method would be used to quantitatively simulate the dynamic axis trajectory change process of the spindle. The influence of factors such as alternating loads, periodic loads, rotor mass, and throttle parameters on the spindle rotation accuracy during the machining process would be studied

2. Dynamic Model of Aerostatic Spindle

2.1. Rotor dynamics model of aerostatic spindle

The aerostatic spindle system is shown in Fig. 1.

The aerostatic bearings have dual row throttling to provide a certain pressure gas. The aerostatic spindle is subjected to gravity, unbalanced load, nonlinear load, and nonlinear film force during operation. The force model of the aerostatic spindle is shown in the Fig. 2.

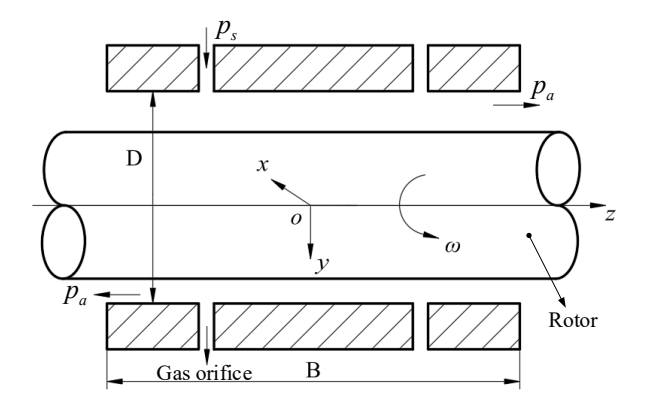


Fig. 1 Schematic diagram of the aerostatic spindle system

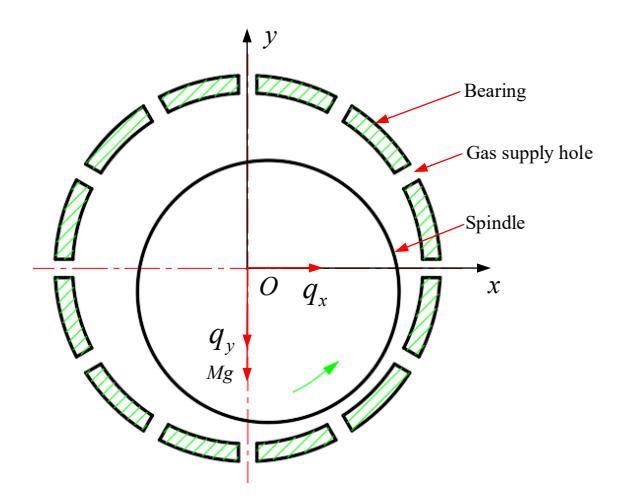


Fig. 2 Aerostatic spindle force model

The motion equation of the aerostatic spindle at any time is expressed as Eq. (1):

$$\begin{cases}
m\ddot{x}_c = F_x + q_x \\
m\ddot{y}_c = F_y + q_y - mg
\end{cases}$$
(1)

where M is the mass of the rotor, F_x and F_y are the x-direction and y-direction air film force components, respectively, q_x and q_y are the unbalanced loads in the x and y directions, x and y are the displacement components of the rotor in the x and y directions, respectively.

When the quality of the spindle is uneven, the spindle generates periodic unbalanced loads due to rotation. The unbalance eccentricity e_g is used to represent the unbalanced load, which is shown in Eq. (2)

$$\begin{cases} q_x = Me_g \omega^2 \cos(\omega t) \\ q_y = Me_g \omega^2 \sin(\omega t) \end{cases}$$
 (2)

The above models are processed into dimensionless form. The following dimensionless parameters are introduced:

$$(x, y) = h_0(X, Y), \quad (\ddot{x}, \ddot{y}) = h_0\omega^2(\ddot{X}, \ddot{Y}), \quad \varepsilon_g = e_g/h_0, \quad \tau = \omega t,$$

 $(F_x, F_y) = RBP_a(\overline{F}_x, \overline{F}_y), g = Gh_0\omega^2, \beta = (RBP_a)/(Mh_0\omega^2).$

The dimensionless form of the spindle motion equation is shown in Eq. (3)

$$\begin{cases}
\ddot{X}(\tau) = \beta \bar{F}_x(\tau) + \varepsilon_g \cos(\tau) \\
\ddot{Y}(\tau) = \beta \bar{F}_y(\tau) + \varepsilon_g \sin(\tau) - G
\end{cases}$$
(3)

2.2. Transient Reynolds equation for orifice throttling

The pressure distribution of the gas film can be solved by the transient Reynolds equation, assuming that the gas flow in the gas film gap is laminar. The transient gas Reynolds equation for orifice throttling is expressed as Eq. (4) [7].

$$\frac{\partial}{\partial x} \left(ph^{3} \frac{\partial p}{\partial x} \right) + \frac{\partial}{\partial z} \left(ph^{3} \frac{\partial p}{\partial z} \right) + 12\eta \rho \frac{p_{a}}{\rho_{a}} \tilde{v} \delta_{i} =
= 6\eta \omega R \frac{\partial (ph)}{\partial x} + 12\eta \frac{\partial (ph)}{\partial t},$$
(4)

where h is the thickness of the gas film, p is a gas pressure, η is a gas viscosity, \tilde{v} is gas flow velocity at the throttle hole. ω is rotor angular velocity, p_a is atmospheric pressure, ρ_a is atmospheric density, δ_i is the Dirichlet function

$$\delta_i = \begin{cases} 0 & \text{position of non throttle hole} \\ 1 & \text{position with throttle hole} \end{cases}.$$

For radial sliding bearings, the transient Reynolds equation can be represented in cylindrical coordinates without dimensional processing $x = R\theta$, $z = b\overline{z}$, $\tau = \omega t$, $p = \overline{p}p_a$, $h = \overline{h}h_0$.

Therefore, the dimensionless transient Reynolds equation is expressed as Eq. (5).

$$\frac{\partial}{\partial \theta} \left(\overline{p} \overline{h}^{3} \frac{\partial \overline{p}}{\partial \theta} \right) + \alpha \frac{\partial}{\partial \overline{z}} \left(\overline{p} \overline{h}^{3} \frac{\partial \overline{p}}{\partial \overline{z}} \right) + Q \delta_{i} =$$

$$= \Lambda \frac{\partial (\overline{p} \overline{h})}{\partial \theta} + 2\Lambda \frac{\partial (\overline{p} \overline{h})}{\partial \tau}. \tag{5}$$

where R is rotor radius, b is bearing length: $Q = \frac{12\eta R^2 p_a}{\rho_a p_a^2 h_0^3} \rho \tilde{v}, \quad \Lambda = \frac{6\eta \omega R^2}{p_a h_0^2}, \quad \alpha = \frac{R^2}{b^2}$

The calculation of gas mass flow rate from a single orifice outlet [12] is shown in Eq. (6)

$$\dot{m} = \phi_{orifice} p_s A \psi \sqrt{\frac{2\rho_a}{p_a}} , \qquad (6)$$

where $\phi_{orifice}$ is the flow coefficient, usually taken as 0.8, A is the area of the throttle hole, k is gas specific heat ratio, usually taken as 1.4 for air, β_k is the critical pressure ratio

$$\beta_{k} = \left(\frac{2}{k+1}\right)^{\frac{k}{k-1}},$$

$$\psi = \begin{cases} \left[\frac{k}{2}\left(\frac{2}{k+1}\right)^{\frac{k+1}{k-1}}\right]^{\frac{1}{2}} & \frac{p}{p_{s}} \leq \beta_{k} \\ \left\{\frac{k}{k-1}\left[\left(\frac{p}{p_{s}}\right)^{\frac{2}{k}} - \left(\frac{p}{p_{s}}\right)^{\frac{k+1}{k}}\right]\right\}^{\frac{1}{2}} & \frac{p}{p_{s}} > \beta_{k} \end{cases}$$

The expression for the film thickness of the rotor at any given time is shown in Eq. (7)

$$h = h_0 + x \sin \theta - y \cos \theta \ . \tag{7}$$

The dimensionless form of Eq. (7) is as shown in Eq. (8)

$$H = \frac{h}{h_0} = 1 + X \sin \theta - Y \cos \theta. \tag{8}$$

3. Numerical Solution of Axial Motion Trajectory of Aerostatic Spindle

3.1. Boundary conditions

The air film gap is generally in the micro meter range, would be ignored relative to the bearing size. Therefore, in the numerical calculation process, the bearing can be unfolded into a plane, as shown in Fig. 3.

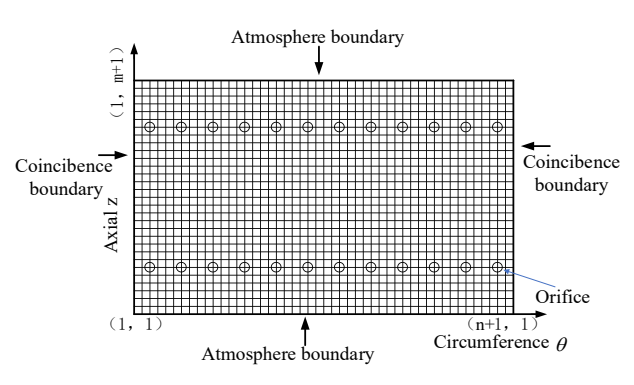


Fig. 3 Schematic diagram of grid division and boundary conditions

The boundary conditions:

The two end faces of the bearing are connected to the atmosphere: $p = p_q$.

Gas film pressure boundary at the orifice: $p = p_d$. Where p_d is the outlet pressure of the throttle hole.

3.2. Numerical calculation

The axial position of the aerostatic spindle is constantly changed by external load excitation. To calculate the trajectory of the spindle axis, it is necessary to simultaneously solve the Reynolds equation and the rotor dynamics equation to obtain the corresponding axis acceleration, velocity, and displacement. Then calculate the axial acceleration, velocity, and displacement at the next moment based on the Euler algorithm. The specific calculation process is shown in Fig. 4.

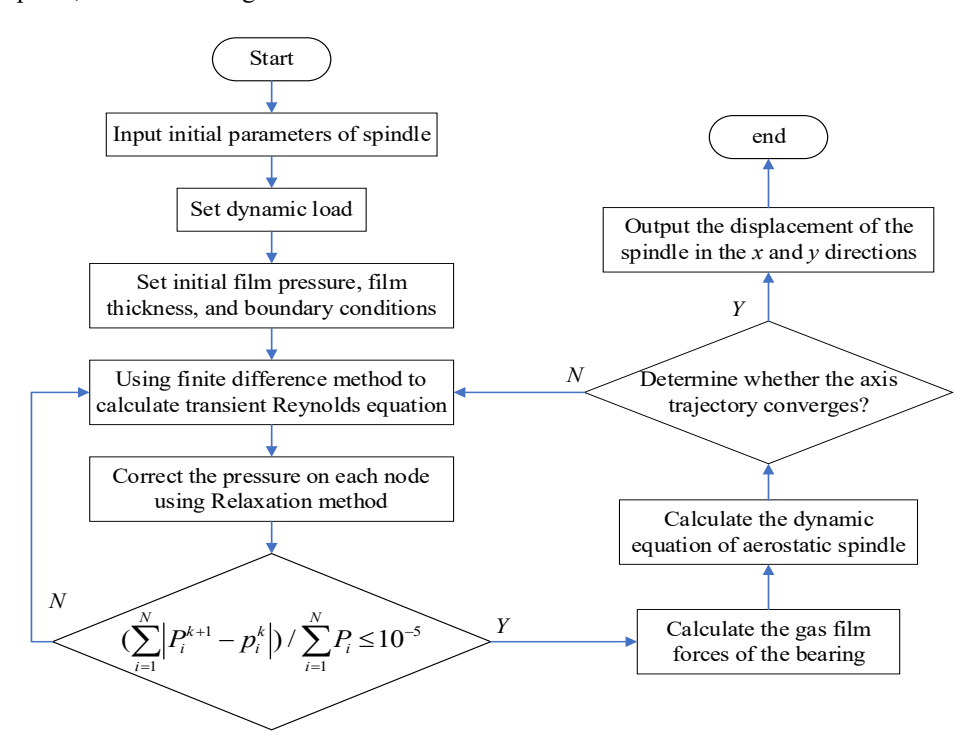


Fig. 4 Flow chart for calculation of axis trajectory of aerostatic spindle

The transient Reynolds equation is solved through continuous iteration, and the gas film field is obtained when the gas film pressure reaches convergence accuracy. The iterative convergence condition is shown in Eq. (9)

$$\frac{\sum \sum \left| \bar{p}_{i,j}^{k+1} - \bar{p}_{i,j}^{k} \right|}{\sum \sum \bar{p}_{i,j}^{k}} \le 10^{-5} \,. \tag{9}$$

By integrating the entire gas film pressure field, the gas film force is obtained as shown in Eq. (10)

$$F_{x} = \int_{0}^{B} \int_{0}^{2\pi R} (p - p_{a}) \sin \theta dx dz$$

$$F_{y} = \int_{0}^{B} \int_{0}^{2\pi R} (p - p_{a}) \cos \theta x dz$$
(10)

4. Analysis of the rotational accuracy laws of the aerostatic spindle

In order to verify the correctness of the paper, the program written by oneself is used to simulate the data in the reference [13] for result comparison. The structural parameters in reference [13] are shown in Table 1.

Table 1

Structural parameters of aerostatic spindle system in reference [13]

Parameter	Value	Parameter	Value
Bearing diameter	16 mm	Rotor length	90 mm
Bearing length	24 mm	Rotor mass	0.14 kg
Orifice diameter	0.3 mm	Unbalanced mass	1 mg, 3mg
Distance between the orifice and the end	6 mm	Eccentric distance	8 mm
Bearing nominal clearance	15 mm	Turbine mass	5 g
Supply pressure	7.5 bar	Compressor	8 g

The comparison of simulation results is shown in the Fig. 5. The bearing structure parameters, gas parameters, and operating parameters of the aerostatic spindle simulated in this article are shown in Table 2. From the comparisons of the axis trajectories in Fig. 5, a and Fig. 5, b, it can be seen that the final stable position of the axis trajectory is highly consistent. Simultaneously, the vibration pattern of the rotor is enormously consistent. The vibration amplitudes in the x and y directions are extremely close. Therefore, the comparison results validate the correctness of the program.

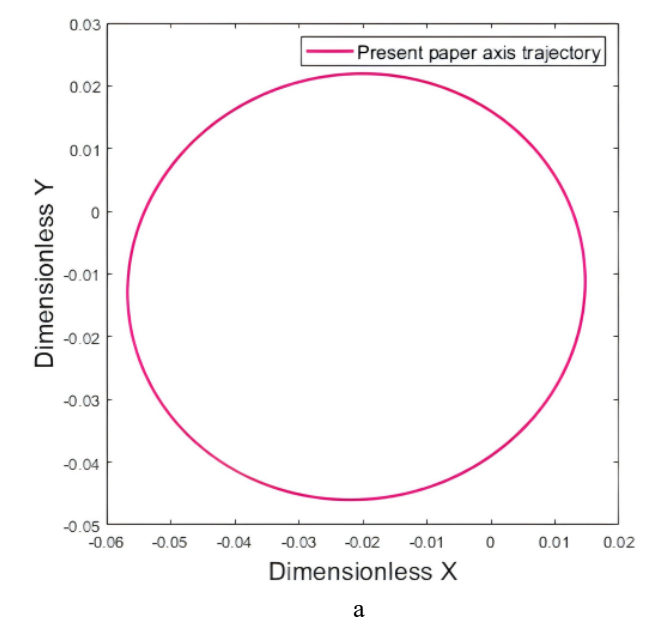
4.1. The influence of periodic load on rotation accuracy

Periodic loads are mainly caused by the unbalance eccentricity of the spindle. The numerical calculations in this article are based on the parameters listed in Table 1. Under the conditions of only self gravity and a rotational speed of 6000 rpm, the rotational accuracy of the aerostatic spindle

is investigated under the conditions of rotor mass eccentricity of 0.4 um, 0.6 um, 0.8 um, and 1 um, respectively.

Table 2
Parameters of aerostatic spindle system

Structure parameters	Numerical value
Bearing length B, mm	80
Bearing radius R, mm	40
The diameter of the small hole d , mm	0.15
Initial film thickness h_0 , μ m	14
Air supply pressure Ps, MPa	0.6
Gas viscosity η, Pa·s	1.82×10 ⁻⁵
Gas density ρ , kg·m ⁻³	1.29
Rotor mass m, kg	13



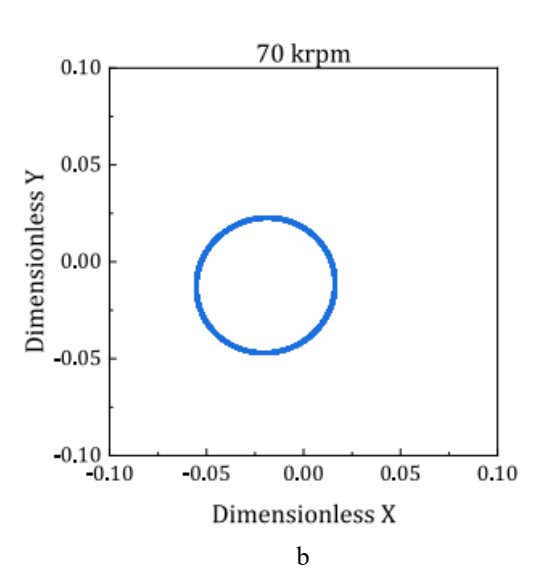


Fig. 5 Verification of axis trajectory model: a – the calculation results of the present program, b – literature results [13]

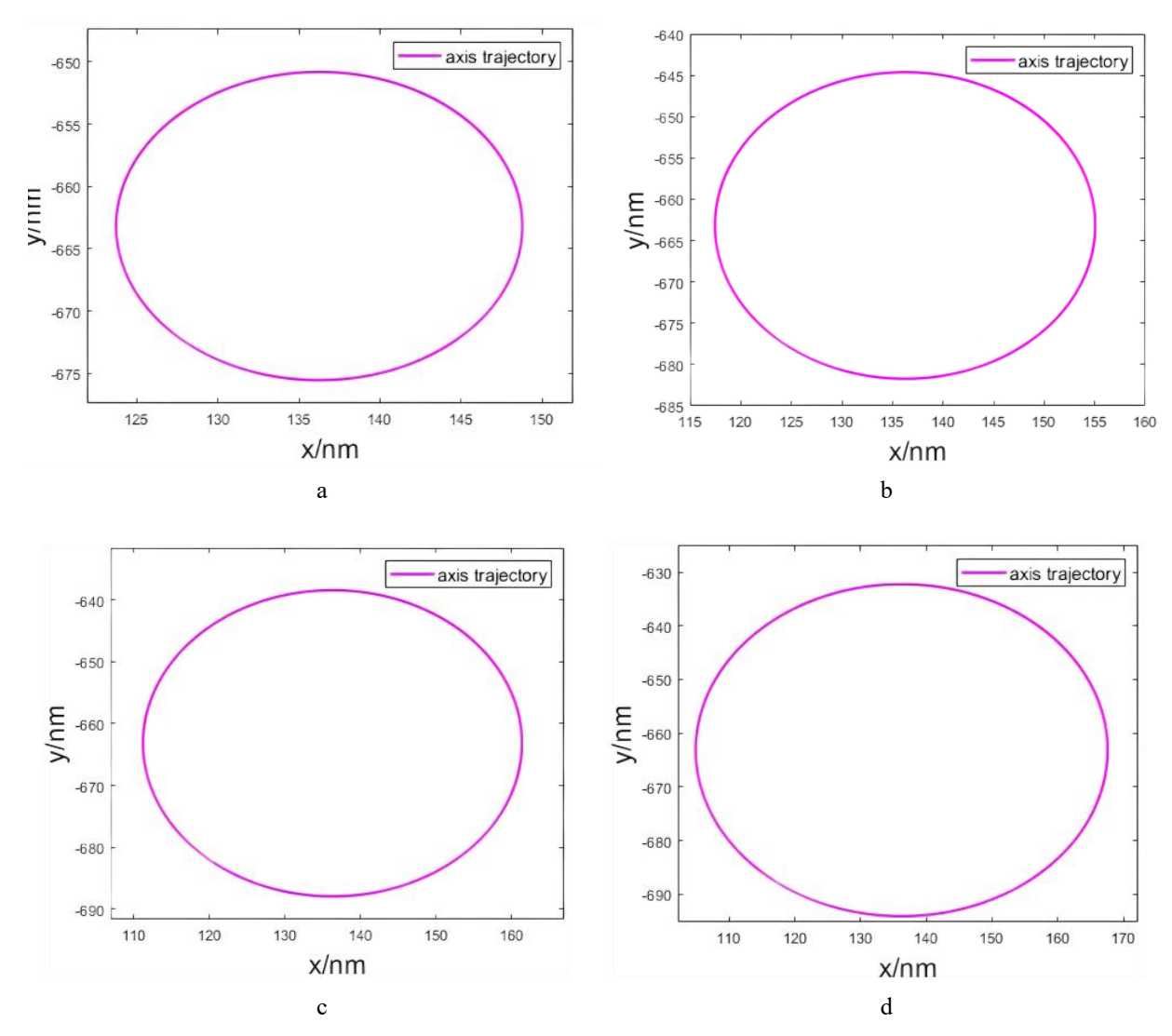


Fig. 6 The influence of rotor unbalance eccentricity on rotational accuracy: a – unbalance eccentricity 0.4 μm, b – unbalance eccentricity 0.6 μm, c – unbalance eccentricity 0.8 μm, d – unbalance eccentricity 1 μm

Table 3
Comparison of spindle vibration amplitudes under different unbalance eccentricities

Unbalance eccentricities, μm	Vibration amplitude in the <i>X</i> direction, nm	Vibration amplitude in the <i>Y</i> direction, nm
0.4	12.53	12.37
0.6	18.80	18.54
0.8	25.07	24.72
1.0	31.33	30.92

According to the analysis in Fig. 6, the vibration amplitude of the aerostatic spindle increases with the increase of the unbalance eccentricity, which seriously affects the rotational accuracy. According to the data in Fig. 6 and Table 3, the final stable shape of the spindle is elliptical, and the vibration amplitude in the x direction is very close to that in the y direction. This indicates that the spindle is in periodic motion and in a stable state. The rotational accuracy increases as the unbalance eccentricity decreases. Therefore, in the design and processing of spindle, it is necessary to perform multi-faceted dynamic balancing to ensure that the spindle has high dynamic balancing accuracy, thereby

improving the rotational accuracy.

4.2. The influence of rotational speed on rotation accuracy

The rotational speed has a significant impact on the rotational accuracy of the aerostatic spindle. The air film excitation and unbalanced centrifugal force caused by increasing of spindle speed will reduce the rotational accuracy. Under the condition of unbalance eccentricity of 0.6 um, the laws of the rotational accuracy of the spindle are investigated at speeds of 4000 rpm, 5000 rpm, 6000 rpm, and 7000 rpm.

Through the analysis of Fig. 7 and Table 4, the rotational speed of the aerostatic spindle directly affects the rotational accuracy. The vibration amplitude of the spindle increases with the increase of the rotational speed, because as the speed increases, the centrifugal force caused by the unbalance eccentricity increases, leading to a decrease in the rotational accuracy. As the rotational speed increases, the balance position of the spindle moves towards the center of the bearing. Due to the increase in rotational speed, the gas dynamic pressure effect is significant, resulting in an increase in gas film force and a decrease in rotor eccentricity. Based on the above data, to achieve high rotational accuracy, it is necessary to ensure the matching relationship

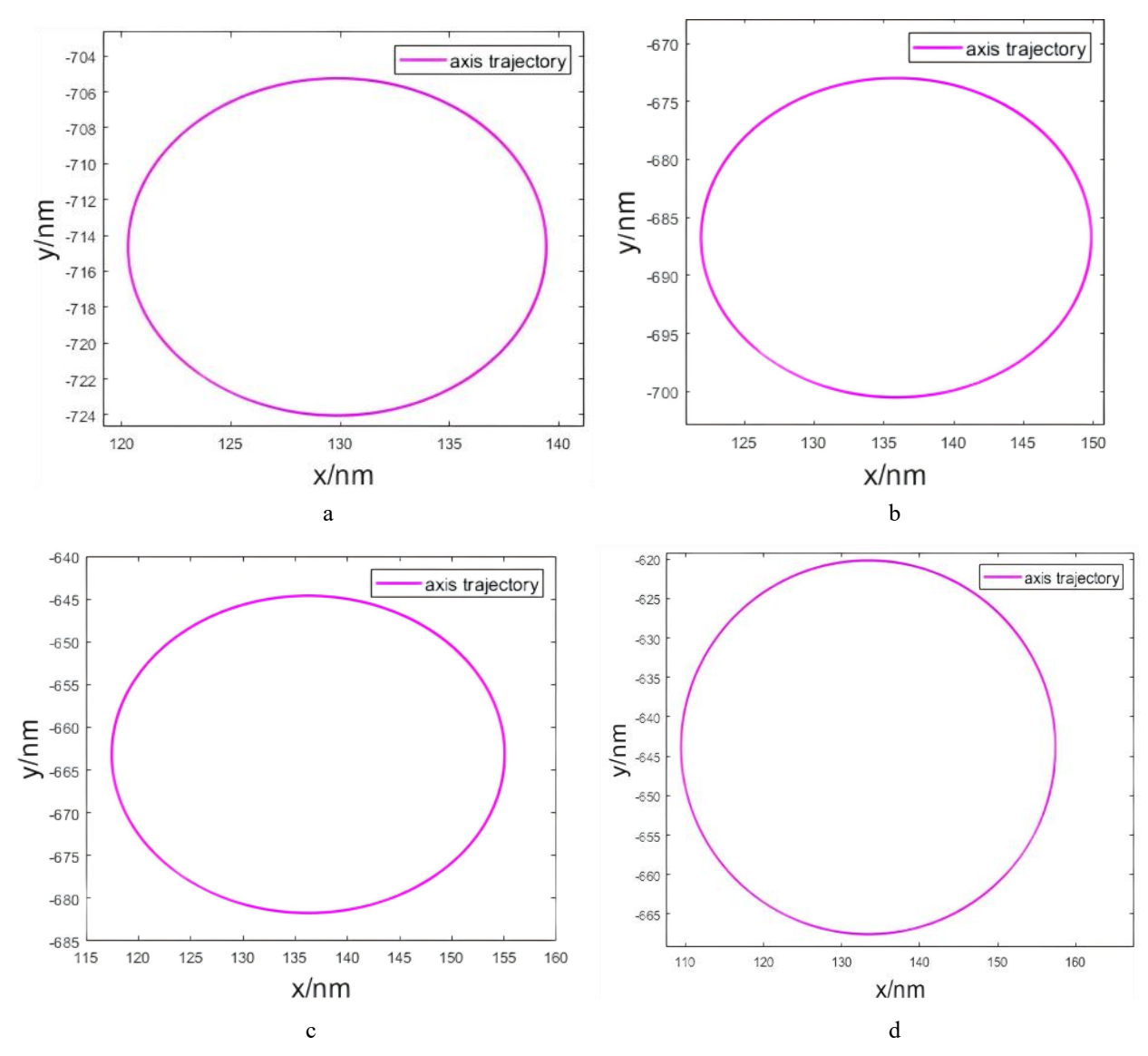


Fig. 7 The influence of different spindle speeds on rotation accuracy: a—rotational speed 4000 rpm, b – rotational speed 5000 rpm, c – rotational speed 6000 rpm, d – rotational speed 7000 rpm

Table 4
Comparison of spindle vibration amplitudes
at different speeds

ar annorm of come				
Rotational speed, rpm	Vibration amplitude in the <i>X</i> direction, nm	Vibration amplitude in the <i>Y</i> direction, nm		
4000	9.55	9.39		
5000	13.96	13.76		
6000	18.80	18.54		
7000	23.98	23.68		

between the structural parameters of the bearing and rotor and the rotational speed in designing the aerostatic bearing rotor system.

4.3. The influence of impact load on rotation accuracy

The aerostatic spindle is not only affected by its own gravity during the actual machining process, but also subjected to certain impact loads and cutting force loads This section sets a fixed load along the direction of gravity, with a magnitude equivalent to the rotor's own gravity. The cutting load simulation is a periodic load. According to engineering cutting experience, the cutting force of a single point diamond lathe is relatively small, so the size of the simulated cutting load is 15% of the rotor gravity. The transition process of the axis trajectory under only cutting load is shown in Fig. 8. The transition process of the axis trajectory under both impact load and cutting load is shown in Fig. 9.

Through the analysis of Fig. 8 and Fig. 9, it is found that the spindle is subjected to impact or cutting loads after initial stability. Next, the trajectory of the spindle axis undergoes dynamic response and then stabilizes at the new equilibrium position. According to the analysis in Fig. 8, the axis balance position of the spindle does not change when only subjected to periodic cutting loads. The vibration amplitudes in the x and y directions increased by 61.98% and 61.95%, respectively. According to the analysis in Fig. 9, when the spindle is subjected to both vertical downward impact load and periodic cutting load, the balance position of the rotor axis would deviate from the center of the bearing and downward movement. Moreover, as the vibration

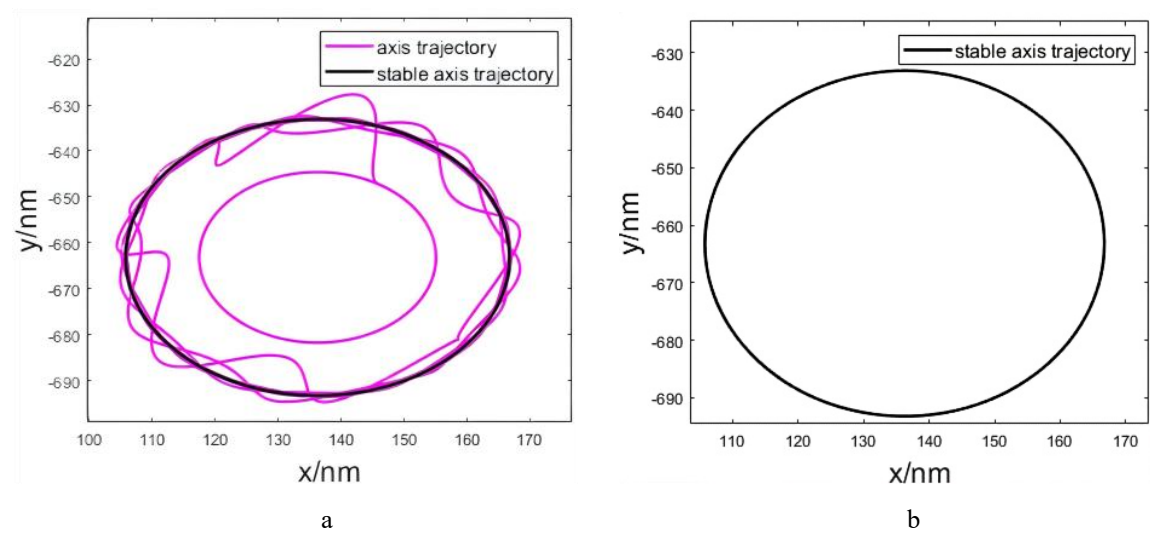


Fig. 8 Transition process of axial trajectory change of spindle under cutting load: a – evolution process of trajectory under cutting load, b – stable trajectory under cutting load

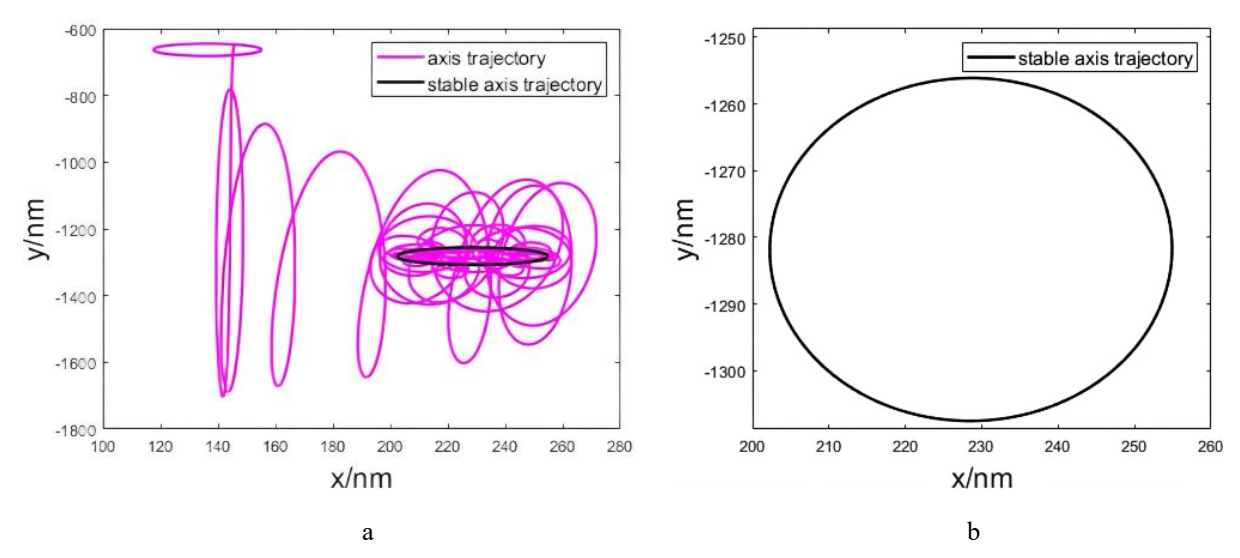


Fig. 9 Transition process of axis trajectory change under impact load and cutting load on the spindle: a – evolution process of trajectory under cutting load and impact load, b – stable trajectory under cutting load and impact load

amplitude increases in both the x and y directions, the rotational accuracy decreases. Therefore, through the above analysis, accurately calculating the impact load and cutting load on the aerostatic spindle during the actual machining process can effectively simulate the rotational accuracy and stable form. It has accurate guidance significance for the design of ultra precision aerostatic spindle. At the same time, it is possible to predict the threshold of the maximum load that the spindle can withstand.

5 Conclusions

This article first has established a dynamic model of the aerostatic spindle. The transient gas Reynolds equation was solved to obtain the gas film pressure. Then, the Euler iterative algorithm was used to obtain the main axis position at each time step. Finally, the influence of unbalance eccentricity, rotational speed, and non periodic loads on the spindle rotation accuracy was analyzed. The conclusions are as follows:

1. The influence of rotor mass imbalance on spindle rotation accuracy has been studied. Research has found that the vibration amplitude of the aerostatic spindle increases with the increase of unbalance eccentricity. When considering only the gravity of the spindle, the vibration amplitude of the spindle in the *x* and *y* directions increased by 14.4 nm and 14.29 nm, respectively, as the spindle unbalance eccentricity increased from 0.4 um to 1um. For the design and processing of ultra precision spindles, it is necessary to perform multi-faceted dynamic balancing on the rotor to maximize the dynamic balancing accuracy, thereby improving the rotational accuracy of the aerostatic spindle.

2. The influence of rotor speed on spindle rotation accuracy has been studied. Research has found that as the rotational speed increases, the vibration amplitude of the spindle gradually increases. When considering only the gravity of the spindle, the vibration amplitude of the spindle in the *x* and *y* directions increased by 14.4 nm and 14.29 nm, respectively, as the spindle speed increased from 4000 rpm to 7000 rpm. Therefore, when designing a high-speed aerostatic spindle with high rotational accuracy, it is necessary to quantitatively simulate the matching relationship between the structural parameters of the aerostatic bearing and the rotor with the rotational speed.

3. The influence of impact load and cutting load on the spindle rotation accuracy and stable form has been studied. Research has found that applying impact and cutting loads to the aerostatic spindle resulted in dynamic response of the spindle axis trajectory. Furthermore, the maximum cutting load should not exceed 15% of the rotor's gravity as much as possible. Ultimately, it led to a change in the balance position of the spindle and a decrease in rotational accuracy. Therefore, accurately simulating the influence of nonlinear loads on the axis trajectory of the aerostatic spindle during actual machining process had guiding significance for improving the spindle rotation accuracy and the maximum load that the spindle can withstand.

References

- 1. Gao, Q.; Chen, W.; Lu, L.; Huo, D.; Cheng, K. 2019. Aerostatic bearings design and analysis with the application to precision engineering: State-of-the-art and future perspectives, Tribology International 135: 1-17. https://doi.org/10.1016/j.triboint.2019.02.020.
- Yu, K. N.; Hsieh, C. T.; Wang, C. C.; Yau, H. T.; Jang, M. J. 2016. Influence of bearing number on high speed air rotor bearing systems, In 2016 IEEE 14th International Conference on Industrial Informatics 1252-1255.

https://doi.org/10.1109/INDIN.2016.7819359.

3. An, L.; Wang, W.; Wang, C. 2023. Dynamic modeling and analysis of high-speed aerostatic journal bearing-rotor system with recess, Tribology International 187: 108686.

https://doi.org/10.1016/j.triboint.2023.108686.

4. Yang, D. W.; Chen, C. H.; Kang, Y.; Hwang, R. M.; Shyr, S. S. 2009. Influence of orifices on stability of rotor-aerostatic bearing system, Tribology International 42(8): 1206-1219.

https://doi.org/10.1016/j.triboint.2009.04.002.

- Zhang, J.; Han, D.; Song, M.; Xie, Z.; Rao, Z.; Zou, D. 2021. Theoretical and experimental investigation on the effect of supply pressure on the nonlinear behaviors of the aerostatic bearing-rotor system, Mechanical Systems and Signal Processing 158: 107775. https://doi.org/10.1016/j.ymssp.2021.107775.
- Cappa, S.; Reynaerts, D.; Al-Bender, F. 2014. Reducing the radial error motion of an aerostatic journal bearing to a nanometre level: theoretical modelling, Tribology Letters 53(1): 27-41. https://doi.org/10.1007/s11249-013-0241-8.
- Yin, T.; Zhang, G.; Du, J.; To, S. 2021. Nonlinear Analysis of Stability and Rotational Accuracy of an Unbalanced Rotor Supported by Aerostatic Journal Bearings, IEEE Access 9: 61887-61900. https://doi.org/10.1109/ACCESS.2021.3075051.
- Chen, D.; Du, X.; Fan, J.; Pan, R.; Sun, K.; Wang, H. 2025. A study of the influence of speed effect on the kinematic behavior of aerostatic spindles, Mechanical Systems and Signal Processing 224: 112224. https://doi.org/10.1016/j.ymssp.2024.112224.
- 9. Sun, Z.; Guan, C.; Xu, H.; Hu, H.; Dai, Y. 2024. The influence of journal's roundness on rotating accuracy of

- aerostatic spindle and precision improvement by time-controlled grinding, Tribology International 197: 109805.
- https://doi.org/10.1016/j.triboint.2024.109805.
- 10. Shimada, K.; Wakabayashi, D.; Shimoyakawa, Y.; Kawada, S.; Miyatake, M.; Yoshimoto, S. 2022. Numerical study on the rotational and machining accuracy of an end-milling process with spindles supported by aerostatic bearings, Proceedings of the Institution of Mechanical Engineers, Part C: Journal of Mechanical Engineering Science 236(20): 10541-10553. https://doi.org/10.1177/09544062221103366.
- 11. Shi, J.; Cao, H.; Maroju, N. K.; Jin, X. 2019. Dynamic Modeling of Aerostatic Spindle With Shaft Tilt Deformation, ASME Journal of Manufacturing Science and Engineering 142(2): 021006. https://doi.org/10.1115/1.4045630.
- 12. Song, L.; Yuan, G.; Zhang, H.; Ding, Y.; Cheng, K. 2022. Non-Linear Dynamic Analysis on Hybrid Air Bearing-Rotor System under Ultra-High Speed Condition, Materials 15(2): 675. https://doi.org/10.3390/ma15020675.
- 13. Qiu, S.; Ke, C.; Li, K.; Zhang, X.; Peng, N.; Liu, L. 2025. Nonlinear dynamic analysis of a novel tangentially supplied aerostatic bearing-rotor system: theory and experiment, Mechanical Systems and Signal Processing 224: 112221.

https://doi.org/10.1016/j.ymssp.2024.112221.

J. Yang, T. Gong, L. Guo, H. Li, J. Wang, M. Zhao, Z. Li

RESEARCH ON THE ROTATIONAL ACCURACY OF AEROSTATIC SPINDLE UNDER VARIABLE LOAD CONDITIONS

Summary

This study aimed to study the influence of variable load conditions on the rotational accuracy of the aerostatic spindle. The dynamic model of aerostatic spindle was established considering the gravity of the spindle, nonlinear air film force, and external applied loads. By solving the dynamic model, the motion trajectory of the spindle axis was obtained. Finally, a quantitative explanation was provided for the rotational accuracy laws of the aerostatic spindle. As the speed and eccentricity of the spindle increase, the vibration of the spindle in the x and y directions gradually increased, and the rotational accuracy of the spindle decreased. The periodic load of simulating cutting load was superimposed on the spindle, which increased the amplitude of spindle vibration and reduced the rotational accuracy of the spindle, but did not affect the balance position of the spindle. The impact load changed the balance position of the spindle without generating rotational errors.

Keywords: aerostatic spindle, dynamic model, periodic load, impact loads, rotational accuracy.

Received May 29, 2025 Accepted October 22, 2025



This article is an Open Access article distributed under the terms and conditions of the Creative Commons Attribution 4.0 (CC BY 4.0) License (http://creativecommons.org/licenses/by/4.0/).